Science Advances
AAAS

Manuscript Template

FRONT MATTER

Title

- Full title: Serial surface mass spectrometry metabolomics on sample-limited tissue archives reveals signatures for predicting pediatric brain tumor relapse (max. 135 characters)
- Short title: Metabolic profiling of pediatric brain tumors (max. 50 characters).

Authors

J. Meurs,[1] D.J. Scurr,[1] A. Lourdusamy,[2] L.C.D. Storer, [2] R.G. Grundy, [2] M.R. Alexander,[1] R. Rahman, [2] D.-H. Kim[1]*

Affiliations

[1] Advanced Materials & Healthcare Technologies Division, School of Pharmacy, University of Nottingham, UK

[2] Children's Brain Tumour Research Centre, Biodiscovery Institute, School of Medicine, University of Nottingham, UK

* Corresponding author. Email: dong-hyun.kim@nottingham.ac.uk

Abstract

Ependymomas are the third most common brain tumor in children and are characterized by a high probability of relapse (>50%) and poor survival rate (<50%). The availability of pediatric ependymoma tissue for analysis is however scarce and small in size (<1 mm) limiting extensive metabolomics analysis into brain tumor metabolism using standard techniques such as gas or liquid chromatography-mass spectrometry and nuclear magnetic resonance spectroscopy. Here, we present a novel serial surface mass spectrometry-based strategy for metabolite profiling of pediatric ependymoma tissue microarrays (TMA) using Orbitrap secondary ion mass spectrometry (3D OrbiSIMS), followed by liquid extraction surface analysis-tandem MS (LESA-MS/MS). The use of this strategy permitted a broader coverage of metabolites and allowed identification of putative metabolites for accurate prediction of ependymoma relapse. This strategy opens new opportunities to retrospectively link molecular data from any formalin-fixed paraffin-embedded (FFPE) TMA library with clinical outcomes.

MAIN TEXT

Introduction

Central nervous system (CNS) pediatric tumors are the most prevalent type of solid cancer diagnosed in children (*1*) and the leading cause of mortality among all cancers in children (*1*). From the clinical and biological perspective, intracranial pediatric ependymomas (pEPNs) remain enigmatic and challenging tumors to treat. Overall, the prognosis is poor with over 50% of tumors relapsing and less than 50% of children surviving this disease (5-year overall survival is ~25% for patients who have relapsed (*2–4*)). Though widely considered a 'surgical disease', a significant proportion of patients relapse, even following complete surgical resection of the tumor. The identification of biological correlates of disease progression and patient-tailored therapeutic targets therefore remains a significant challenge in this disease. Understanding the biochemical nature of tumor development is of vital importance for the development of the next-generation of treatments (*2*). In a disease state, the human metabolome is affected by several factors and therefore provides an excellent source of information to investigate disease-related alterations in metabolism (*5*). To do so, an untargeted metabolomics approach can be used to study molecular changes within and between tissue samples of different phenotypes (*6*, *7*). State-of-the-art metabolomics techniques allow the detection of hundreds to thousands of metabolites in a biological sample (*8*), where untargeted metabolomics of cancer tissue is undertaken using liquid chromatography-mass spectrometry (LC-MS) and gas chromatography-MS (GC-MS) (*9*, *10*). Chromatography-based strategies allow the identification of a vast number of metabolites; however, these require 20-50 mg of tissue for metabolomics analysis.

Preserving tumor regions of interest is commonly achieved using the tissue microarray (TMA) format. The neuropathologist identifies and cuts out key regions in the whole tissue section which are stored as a separate formalin-fixed paraffin-embedded (FFPE) block. The TMA platform allows small amounts of tissue to be used for transcriptomic and histological analysis (*11–13*), though for diagnosis the entirety of the tumor needs to be reviewed. Since the TMA tissue sections are small (diameter <1 mm; thickness: 4 µm), sensitive analytical techniques are required for metabolomic studies to detect low-abundance metabolites. Despite the vast amount of available TMA libraries, metabolite profiling of tumor TMAs has been an unexplored territory due to incompatibility of LC-MS or GC-MS analysis. In order to perform MS analysis on TMAs, a technique is required to directly obtain a wide range of metabolites from small tissue sections.

A few studies have shown the potential of liquid extraction surface analysis-MS (LESA-MS) for untargeted metabolomics across a range of sample types. With LESA-MS, liquid microjunction-based extraction can be performed on a flat sample surface to obtain the analytes of interest which are directly injected into the mass spectrometer (*14*). Hall *et al.* (*15*) found significantly changed profiles of lipids in non-alcoholic fatty liver disease (NAFLD) tissue using LESA-MS. This allowed discrimination between different stages of stearosis. Ellis *et al.* (*16*) used LESA-MS for the analysis of single-cell arrays and could distinguish cell types based on lipid profiles showing the capability of performing single-cell metabolomics with LESA. We have also successfully used LESA-MS to identify metabolic changes in small volumes of urine samples from an intervention study (*17*). Basu *et al.* (*18*) used LESA-MS for direct metabolite profiling for several different breast cancer cell lines. The capability of LESA was shown to allow direct analysis of adherent cells with minimal sample preparation. Collectively, these studies have shown that from a limited amount of sample, metabolic changes could be measured accurately.

The recent development of Orbitrap secondary ion MS (3D OrbiSIMS) revealed new possibilities for metabolic profiling due to its capability of high mass accuracy and mass resolving power (>240,000 at m/z 200) at subcellular spatial resolution (*19*). In that study, it was shown that 3D OrbiSIMS can be used for 2D and 3D imaging of neurotransmitters, in situ identification of lipid species using tandem MS, and performing metabolomics profiling of single cells (*19*). One unmet scientific challenge for brain tumor research is the capability to perform metabolomics analysis on archived TMAs to understand tumor development and find potential targets for therapies (*8*, *20*).

It has been reported that MS is not the preferred method of choice for *ex vivo* metabolomics on brain tumors due to the requirement to extract the metabolites for analysis which prevents subsequent analysis of the valuable sample (*1*). 3D OrbiSIMS and LESA tandem MS (LESA-MS/MS) require only minimal sample preparation, analysis can be performed directly on the tissue sample, and both instruments can acquire data in an automated manner using the TMA sample platform. These MS techniques can therefore circumvent the need for tissue homogenization, allowing the tissue to remain architecturally intact and available for subsequent study. The data achievable using this approach will address current challenges in cancer metabolomics, as detection of low abundance (highly polar) oncometabolites to study important metabolic pathways, may enable the development of novel prognostic and treatment strategies (*9*, *21*). To date, no disease studies have thus far reported the use of combined 3D OrbiSIMS and LESA-MS/MS for untargeted metabolite profiling on TMAs. Combining MS techniques, in which ions are generated via different mechanisms, will allow acquisition of complementary metabolomic datasets from the same set of samples. Combination of the individual datasets on existing TMA archives could therefore provide a vast amount of clinically valuable information. Here, we perform 3D OrbiSIMS and LESA-MS/MS analysis of FFPE pediatric

ependymoma TMAs as an exemplar demonstration of the ability to perform untargeted surface metabolomics and obtain clinically relevant data.

Results

Predicting tumor recurrence from fused metabolite profiles

De-paraffinized ependymoma TMA samples (**Fig. 1**A-B and **Fig. S1**) were analyzed with 3D OrbiSIMS (**Fig. 2**C) followed by LESA-MS/MS (**Fig. 1**D) and processed using a custom MATLAB script for peak picking, alignment, data fusion and multivariate analysis (**Fig. 1**E-F). To investigate the potential of the serial MS strategy with data fusion (combining individual datasets for multivariate analysis) for oncometabolomics, samples were categorized by eventual tumor recurrence. Since complementary metabolite profiles were obtained with individual techniques (**Fig. S2**), data fusion and multivariate analysis assisted in the discovery of complementary and novel discriminative metabolites between no relapse and eventual relapse ependymoma tumors. Furthermore, prior analysis by 3D OrbiSIMS did not lead to a decrease in either the number of detected ions (Student's *t*-test: $p = 0.2578$) or ion intensity (Student's *t*-test: $p = 0.1806$) for LESA-MS/MS data (**Fig. S3**), indicating that subsequent metabolite profiling with LESA-MS/MS can be performed without data loss. Analyzed tumor sections consisted of 7 primary tumors with each of three replicates, though for 5 out of 7 patients in this dataset, the tumor recurred at least once after surgery or follow-up treatment (**Table 1**).

Through data fusion and multivariate analysis (partial least squares-discriminant analysis (PLS-DA)), we were able to cluster patients based on eventual tumor recurrence (**Fig. 2**A). After PLS-DA, the model was validated using leave-one-out cross validation which resulted in a Q^2 (goodness-of-prediction) of 0.4334. Through a permutation test *(22)*, it was shown that no random PLS-DA model predicted tumor recurrence better than the original PLS-DA model ($p < 0.05$). To identify the discriminative ions between no relapse and eventual relapse ependymoma cohorts, the variable's importance in projection (VIP) score for each ion was calculated. A VIP score ≥ 1.5 was considered discriminative. The ions which met this criterion were subjected to Student's t-test to determine which ions were significantly altered between the two groups. In total, we identified 27 significant mass ions ($p < 0.05$; **Fig. 2**B). From those 27 mass ions, 18 mass ions were assigned putative molecular formulae using the Human Metabolome Database (**Table 2**) *(23)*. Most of the significant ions were found to be more prominent in the no relapse group.

The molecular information was used in MetExplore (24) for the identification of putative metabolite IDs and their corresponding metabolic pathways and genes (**Table 3**). Through pathway analysis, we were able to identify four pathways that were significantly altered ($p < 0.05$) between the no relapse and eventual relapse groups: tyrosine metabolism, linoleate metabolism, cytochrome metabolism, and phenylalanine metabolism.

The putatively identified genes related to the significant metabolic pathways determined from the metabolomics data were analyzed to test for distinguishing primary tumors from recurrent ones at the gene expression level. We used gene expression data set of primary ($n = 72$) and recurrent ($n = 47$) ependymoma from previously published studies *(25, 26)*. Ten out of the fourteen genes were present, of which four genes showed a significant differential expression (ADHFE1: $p = 0.00234$; GSTK1: $p = 0.00450$; GOT2: $p = 0.0393$; EPHX2: $p = 0.0433$) between primary and recurrent ependymoma. In addition, the group of ten genes as a single gene set showed significant change between primary and recurrent ependymoma ($P = 0.00257$, global test) and showed clear separation of primary tumors from recurrent ependymal tumors (**Fig. 3**).

Discussion

From a prognostic and therapeutic perspective, it is of interest to predict if patients will experience tumor relapse or if primary treatment is successful so therapy can be adjusted consequently. We found several candidate markers which were putatively annotated. Due to the limited availability of ependymoma samples, only a small cohort could be analyzed. We recognize the need for an increase in the number of patients to validate these results, though the data shows the clinical potential for the serial MS strategy to be further used for metabolomics screening of ependymoma TMAs.

With the use of data fusion and multivariate analysis, we were able to cluster patients based on eventual tumor recurrence. Waziri et al. *(27)* did not find any relation between ependymoma recurrence and demographic factors, tumor grade and location. The PLS-DA model showed an acceptable Q^2 (>0.4) for a biological model *(28)*. Previous work on metabolite profiling of ependymoma via NMR showed that L-phenylalanine is highly abundant and an important discriminative metabolite for ependymoma among other pediatric brain tumors *(1, 29)*. Here, we found a more prominent abundance of L-phenylalanine (*m/z* 146.0610; fold change: 2.53) in the no relapse group. We also identified tryptophan metabolism as a significantly affected pathway between the no relapse and eventual relapse ependymoma cohorts. Previous work has identified phenylalanine and tryptophan metabolism to be important

pathways in brain tumor metabolism *(9)*. This indicates that with the serial MS strategy we can identify important metabolic changes in relation to brain tumors from small amounts of tissue in a high throughput manner. However, these findings need to be validated using a larger patient cohort to characterize the ependymoma metabolite profile for different phenotypes and to confirm the clinical value.

Furthermore, the putatively identified metabolites were known to be associated with a total of 14 genes. Some studies have compared primary and recurrent tumors at the transcriptomic level *(27, 30–32)*. The 14 genes identified in this study were not reported to be significantly altered between primary and recurrent ependymoma in previous transcriptomic research. This could be explained by the fact that all tumors in our study were primary, from which five patients eventually relapsed. From our data, we could hypothesize that the metabolite profiles of primary non-recurrent and primary recurrent ependymoma are different, but primary non-recurrent ependymomas do not reflect the metabolite profile of recurrent ependymoma. Potentially, the metabolite profile, as well as the gene expression profile, become affected by received chemo- and/or radiation therapy.

Linoleate metabolism was upregulated in the eventual relapse group for the conversion of epoxy fatty acids (EpOMEs) to fatty acids and vice versa. Whilst linoleate metabolism has not been reported as an affected pathway for ependymoma relapse, fatty acid oxidation pathways have been reported to be affected in cancer metabolism *(33, 34)*. The putatively identified amino acid metabolism pathways (tryptophan, tyrosine, and phenylalanine) were all downregulated in the eventual relapse group. Also, those pathways have not specifically been reported for ependymoma, though the importance of amino acid metabolism pathways has been recognized for targeting cancer treatment development *(35, 36)*.

The genes identified through direct MS-based metabolomics could be used to classify primary and recurrent ependymoma with good accuracy based on the gene expression profiles. Although the sample size for the MS analysis was limited, the gene expression results from a large data set confirm that the associated genes identified through metabolomics analysis bear predictive value for ependymoma recurrence. This could have a huge impact on the development of personalized therapies and for continued health monitoring using direct MS-based metabolomics as a tool for early prediction of tumor relapse and the identification of cancer vulnerabilities. This may expediate the consideration of new potential therapeutic opportunities at the primary tumor stage, which may prevent or delay recurrence.

Collectively, serial 3D OrbiSIMS and LESA-MS/MS analysis shows to be a versatile analysis strategy for ependymoma FFPE TMA samples. This will permit the retrospective analysis of the vast amount of TMA archives for metabolomics studies with confirmation of findings based on publicly available gene expression datasets. Furthermore, the minimally required sample preparation and short analysis time will allow high sample throughput, making this strategy a competitive alternative to standard metabolomics analysis such as GC-MS, LC-MS and NMR.

Materials and Methods

Experimental design

Hematoxylin and eosin-stained sections from FFPE pediatric ependymoma were examined by a neuropathologist at Nottingham University Hospital, and three representative areas were marked on the slides. Using a Raymond Lamb tissue micro-arrayer, 1 mm cores were punched from the marked areas of the donor blocks and placed into recipient paraffin blocks to generate a tissue microarray (TMA). 4-µm sections were cut from each block for use in further experiments. The analyzed TMA blocks consisted of patients which experienced tumor relapse (N = 5; n =3) and patients without relapse (N = 2; n = 3).

Sample preparation for MS analysis

Deparaffinization of FFPE pediatric ependymoma TMAs was achieved using an adapted protocol from Ly *et al.* (*37*). FFPE TMAs were first washed twice for 1 minute in a xylene bath (mixture of isomers; ≥98.5%, AnalaR NORMAPUR®, VWR, Leicestershire, UK). Residual xylene was removed and the array was allowed to dry in a fume hood for at least one hour, prior to storage at room temperature until analysis.

3D OrbiSIMS

The TMA was placed in a hybrid TOF.SIMS 5 (IONTOF GmbH, Münster, DE) instrument coupled to a Q Exactive HF (Thermo Scientific, San Jose, CA) mass spectrometer. Ions were sputtered from the surface using a 20 keV Ar_{3000}^{+} gas cluster ion beam (GCIB). The field of view (FoV) was set to 500 µm × 500 µm. Spectra were acquired at a resolution of 20 µm in random raster mode. The Orbitrap was operated in Full-MS mode. The resolution was set to 240,000 at *m/z* 200 and the AGC target was set to 1×10^6 with a maximum ion injection of 511 ms. Data were acquired in the scan range *m/z* 75-1125 for both positive and negative polarity.

LESA-MS/MS

The TMA was placed on a universal plate holder (Advion Biosciences, Ithaca, NY) and scanned with an Epson V330 scanner. The tissue sample location was selected in LESA Points (Advion Biosciences, Ithaca, NY). Liquid extraction surface analysis-tandem mass spectrometry (LESA-MS/MS) was carried out using a TriVersa Nanomate (Advion Biosciences, Ithaca, NY) coupled to a Q Exactive plus Orbitrap mass spectrometer (Thermo Scientific, San Jose, CA). Extraction of metabolites from tissue samples was conducted with a mixture of 80% v/v methanol (CHROMASOLV®; Sigma-Aldrich, Gillingham, UK), and 20% v/v water (CHROMASOLV®; Sigma-Aldrich, Gillingham, UK) to which MS-grade formic acid (Optima™ LC-MS grade; Fisher Scientific, Loughborough, UK) was added (end concentration 1% v/v). Brain tissue was sampled using the contact LESA approach (38) in which the solvent tip is brought into contact with the sample to minimize the solvent spread. During contact, 1.5 µL solvent (total volume: 3 µL) was dispensed on the tissue and after 15 seconds, 2.0 µL was aspirated back into the tip. The extract was introduced into the mass spectrometer via chip-based nanoelectrospray ionization (ESI Chip™, Advion Biosciences, Ithaca, NY) at 1.4 kV and 0.3 psi gas pressure (*17*). The mass spectrometer was operated in Full-MS/dd-MS2 mode. MS1 spectra were acquired in the scan range of m/z 70-1050. The resolution was set to 140,000 at *m/z* 200 and the AGC target was set to 3×10^6 with a maximum ion injection time of 200 ms. Data-dependent MS/MS spectra were acquired at a resolution of 17,500 at *m/z* 200. The AGC target for MS^2 scans was set to 1×10^5 with a maximum ion injection time of 50 ms. The top 20 most intense ions were isolated within a 1 *m/z* window for fragmentation. Dynamic exclusion was applied for 120 seconds per polarity. Fragmentation was carried using higher-energy collisional dissociation (HCD) using a stepped collision energy of respectively 10, 25 and 40 eV. All tissue sections were analyzed once. MS data were acquired for 2 minutes per polarity.

Ion selection for multivariate analysis

LESA-MS spectra were averaged in XCalibur (Thermo Scientific, San Jose, CA) and exported in .RAW format. 3D OrbiSIMS spectra were exported from SurfaceLab (IONTOF GmbH, Münster, DE) as .TXT files. Mass spectrometry data were further processed using MATLAB (R2017a, The MathWorks, Inc., Natick, MA; https://github.com/jorismeurs/LESAMS). For LESA-MS data, files were first converted to .mzXML (32-bit) using ProteoWizard 3.0.1908 *(39)*. Ions were selected from the spectra using the mspeaks function and ions were aligned within 5 ppm m/z tolerance (*15*). Ions with >20% missing values across all samples were removed. Remaining missing values were imputed using *k*-nearest neighbor (*k*nn) imputation. The value of *k* was set to 10 (*40*).

Multivariate analysis and pathway analysis

Ion intensity matrices were TIC normalized, log-transformed, and fused using a low-level strategy *(41)*. Processed matrices were subjected to PLS-DA with leave-one-out cross-validation. The PLS-DA model was further validated using permutation testing (*22*). Ions with a VIP score greater than 1.5 were considered discriminative and included for univariate statistical analysis. Significant ions were annotated using the Human Metabolome Database (3 ppm mass tolerance) (*23*). Significant annotated ions were submitted for pathway analysis in MetExplore (*24*).

Gene expression analysis

Two independent gene expression datasets from previously published studies were used for this analysis *(25, 26)*. The first cohort comprised of 65 tumor samples taken at the diagnosis as well as at relapse from 45 pediatric ependymoma patients. Transcriptomic microarray profiles of tumor samples were generated using Affymetrix HG-U133 Plus 2 GeneChip microarrays (Affymetrix, Santa Clara, CA). Expression intensity values were calculated at probeset level from microarray data CEL files using the robust multi-array average (RMA) method. Probesets that are 'absent' (present/absent call using MAS5) in all samples were filtered out from the analysis. Expression values were mapped from probeset to unique gene and the probeset with the highest mean expression value was selected when multiple probesets were mapped to the same gene. The second cohort comprised of 54 tumor samples (both primary and relapse) from 17 pediatric ependymoma patients and profiled with whole-human-genome 44K oligonucleotide microarrays (Dual Color 44K microarray, Agilent Technologies). Raw intensities were background corrected and normalized with a Lowess normalization method for within-array and quantile normalization for between-array normalization *(42)*. The normalized expression values were mapped to unique gene and the probe with the highest mean expression value was selected when multiple probes were mapped to the same gene. The normalized gene expression data from two studies were combined using ComBat, a robust empirical Bayes regression method *(43)*. The differential expression analysis between the primary and recurrent tumors with the ten candidate genes was performed with the moderated t-test and the gene set analysis was performed with the Global test *(44)*.

Statistical analysis

Univariate comparison between ependymoma two subgroups was done using Student's *t*-test. The false discovery rate was estimated through permutations. A p-value less than 0.05 was considered to be significant. All statistical calculations were performed in MATLAB R2017a.

H2: Supplementary Materials

Fig. S1. Example of an ependymoma tissue microarray after deparaffinization
Fig. S2. Identifying putative metabolite features in 3D OrbiSIMS and LESA-MS spectra.
Fig. S3. Investigating the effect of 3D OrbiSIMS analysis on subsequent LESA-MS/MS analysis

References and Notes

1. C. D. Bennett *et al.*, *Sci. Rep.* **8**, 11992 (2018).
2. J.-P. Kilday *et al.*, *Mol. Cancer Res.* **7**, 765–786 (2009).
3. J. Wu, T. S. Armstrong, M. R. Gilbert, *Neuro. Oncol.* **18**, 902–913 (2016).
4. B. Messahel *et al.*, *Eur. J. Cancer*. **45**, 1815–1823 (2009).
5. P. Miggiels, B. Wouters, G. J. P. van Westen, A.-C. Dubbelman, T. Hankemeier, *TrAC Trends Anal. Chem.* (2018), doi:10.1016/J.TRAC.2018.11.021.
6. A. Sreekumar *et al.*, *Nature*. **457**, 910–914 (2009).
7. Q. Huang *et al.*, *Cancer Res.* **73**, 4992–5002 (2013).
8. R. Beger, *Metabolites*. **3**, 552–574 (2013).
9. R. Pandey, L. Caflisch, A. Lodi, A. J. Brenner, S. Tiziani, *Mol. Carcinog.* **56**, 2355–2371 (2017).
10. C. H. Johnson, J. Ivanisevic, G. Siuzdak, *Nat. Rev. Mol. Cell Biol.* **17**, 451–459 (2016).
11. J. Kononen *et al.*, *Nat. Med.* **4**, 844–847 (1998).
12. M. A. Rubin, R. Dunn, M. Strawderman, K. J. Pienta, *Am. J. Surg. Pathol.* **26**, 312–319 (2002).
13. H. Battifora, *Lab. Investig.* **55**, 244–248 (1986).
14. V. Kertesz, G. J. Van Berkel, *J. Mass Spectrom.* **45**, 252–260 (2010).
15. Z. Hall, Y. Chu, J. L. Griffin, *Anal. Chem.* **89**, 5161–5170 (2017).
16. S. R. Ellis *et al.*, *Anal. Chem.* **84**, 9679–9683 (2012).

17. J. Meurs *et al.*, *Anal. Chem.* **90**, 6001–6005 (2018).
18. S. S. Basu *et al.*, *Anal. Chem.* **90**, 4987–4991 (2018).
19. M. K. Passarelli *et al.*, *Nat. Methods*. **14**, 1175–1183 (2017).
20. D. Beyoğlu, J. R. Idle, Metabolomics and its potential in drug development. *Biochem. Pharmacol.* **85** (2013), pp. 12–20.
21. M. Verma, M. J. Khoury, J. P. A. Ioannidis, Opportunities and challenges for selected emerging technologies in cancer epidemiology: Mitochondrial, epigenomic, metabolomic, and telomerase profiling. *Cancer Epidemiol. Biomarkers Prev.* **22** (2013), pp. 189–200.
22. J. A. Westerhuis *et al.*, *Metabolomics*. **4**, 81–89 (2008).
23. D. S. Wishart *et al.*, *Nucleic Acids Res.* **46**, D608–D617 (2018).
24. L. Cottret *et al.*, *Nucleic Acids Res.* **46**, W495–W502 (2018).
25. L. M. Hoffman *et al.*, *Acta Neuropathol.* **127**, 731–745 (2014).
26. M. Peyre *et al.*, *PLoS One*. **5** (2010), doi:10.1371/journal.pone.0012932.
27. A. E. Waziri *et al.*, *J Immunol Ref.* **183**, 7428–7440 (2009).
28. B. Worley, R. Powers, *Curr. Metabolomics*. **1**, 92–107 (2013).
29. S. Cuellar-Baena *et al.*, *Int. J. Mol. Med.* **26**, 941–948 (2010).
30. A. M. Donson *et al.*, *J. Immunol.* **183**, 7428–7440 (2009).
31. S. J. Liu *et al.*, *Cell Rep.* **30**, 1300-1309.e5 (2020).
32. K. A. Michealraj *et al.*, *Cell*. **181** (2020), doi:10.1016/j.cell.2020.04.047.
33. C. S. Yeh *et al.*, *Cancer Lett.* **233**, 297–308 (2006).
34. Q. Qu, F. Zeng, X. Liu, Q. J. Wang, F. Deng, Fatty acid oxidation and carnitine palmitoyltransferase I: Emerging therapeutic targets in cancer. *Cell Death Dis.* **7** (2016), pp. e2226–e2226.
35. R. C. Geck, A. Toker, Nonessential amino acid metabolism in breast cancer. *Adv. Biol. Regul.* **62** (2016), pp. 11–17.
36. M. J. Lukey, W. P. Katt, R. A. Cerione, Targeting amino acid metabolism for cancer therapy. *Drug Discov. Today*. **22** (2017), pp. 796–804.
37. A. Ly *et al.*, *Nat. Protoc.* **11**, 1428–1443 (2016).
38. N. J. Martin, R. L. Griffiths, R. L. Edwards, H. J. Cooper, *J. Am. Soc. Mass Spectrom.* **26**, 1320–1327 (2015).
39. D. Kessner, M. Chambers, R. Burke, D. Agus, P. Mallick, *Bioinformatics*. **24**, 2534–2536 (2008).
40. R. Di Guida *et al.*, *Metabolomics*. **12**, 93 (2016).
41. V. Pirro *et al.*, *Anal. Chim. Acta*. **848**, 51–60 (2014).
42. G. K. Smyth, T. Speed, *Methods*. **31**, 265–273 (2003).
43. W. E. Johnson, C. Li, A. Rabinovic, *Biostatistics*. **8**, 118–127 (2007).
44. J. J. Goeman, S. Van de Geer, F. De Kort, H. C. van Houwellingen, *Bioinformatics*. **20**, 93–99 (2004).

Acknowledgments

Funding: This work was supported by the Engineering and Physical Sciences Research Council [grant number: EP/N006615/1]; grant name: EPSRC Programme Grant for Next Generation Biomaterials Discovery

Author contributions: DHK and RR conceived the study. LCDS prepared the tumor microarrays. JM, DJS and DHK designed the experiments. JM prepared the samples for analysis, performed LESA-MS/MS analysis, processed the data and wrote the manuscript. DJS performed 3D OrbiSIMS analysis. AL performed bioinformatics analysis on the gene

expression data. DHK, RR and MRA supervised the project. DHK, DJS and MRA advised on analytical interpretation of the data. RR and RGG advised on clinical interpretation of the data. All authors read, edited, and approved the manuscript

Competing interests: None

Data and materials availability: The raw and processed data presented in this paper are available through the Nottingham Research Data Repository

Figures and Tables

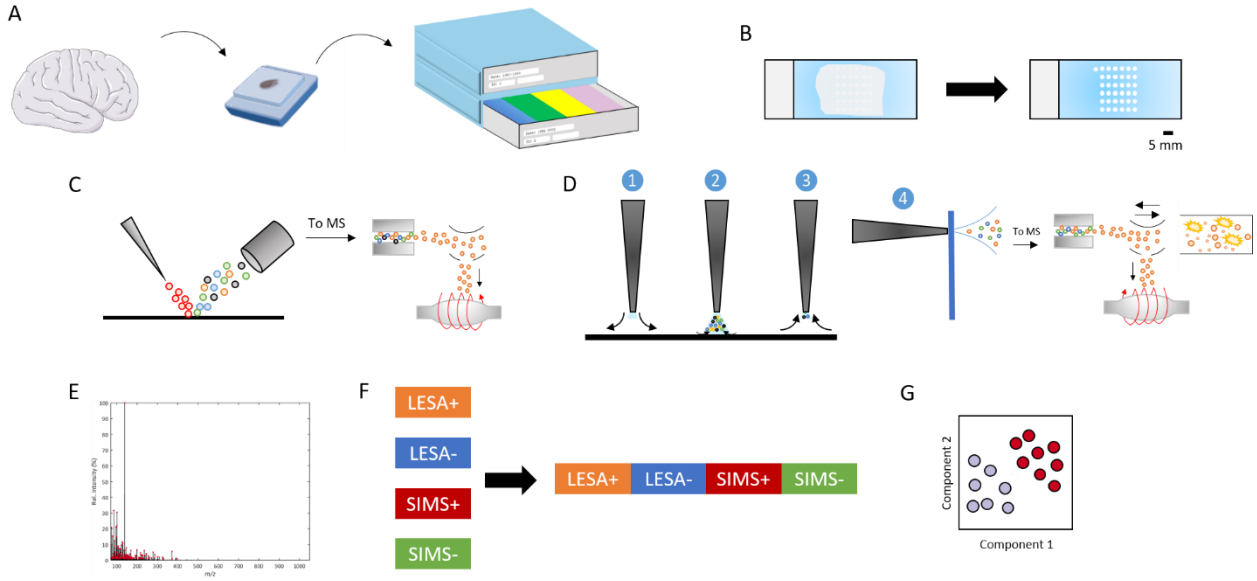

Fig. 1. Serial mass spectrometry analysis of pediatric ependymoma tissue microarrays. (**A**) The tumor tissue is removed, the tumor area is marked and then paraffin-embedded for long term storage. (**B**) For MS analysis, a TMA block from the archive is sectioned and mounted onto a glass substrate followed by a xylene wash to remove the paraffin. (**C**) Paraffin-free samples are then analyzed by OrbiSIMS followed by (**D**) LESA-MS/MS. (**E**) Ions are selected from the mass spectra and aligned. (**F**) All matrices with ion intensities are then combined (low-level data fusion). (**G**) Subsequently, data are subjected to partial-least squares-discriminant analysis (PLS-DA) to identify discriminative features in tumor recurrence.

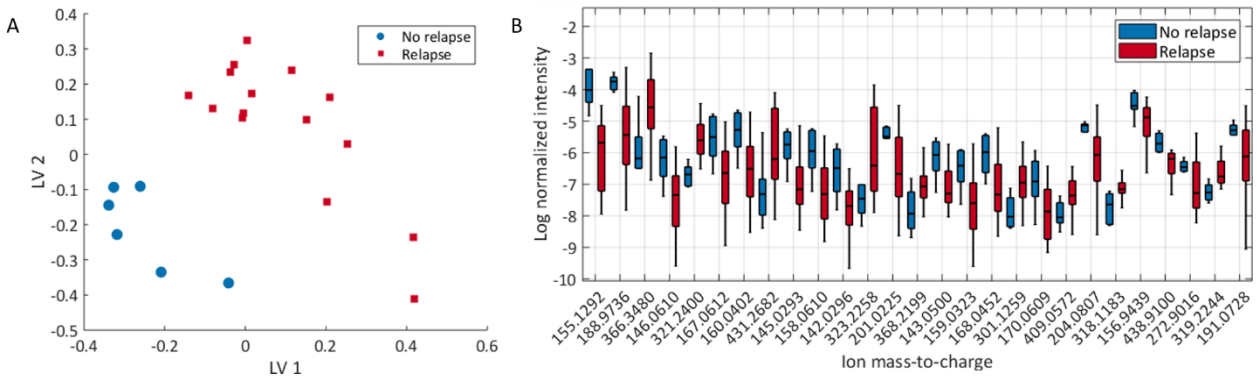

Fig. 2. Identification of significant ions from fused LESA-MS/MS and 3D OrbiSIMS data. (**A**) PLS-DA scores plot reveals clustering of patients based on tumor recurrence. (**B**) Box plot for significant ions ($p < 0.05$) identified using Student's *t*-test and FDR estimation through a permutation test.

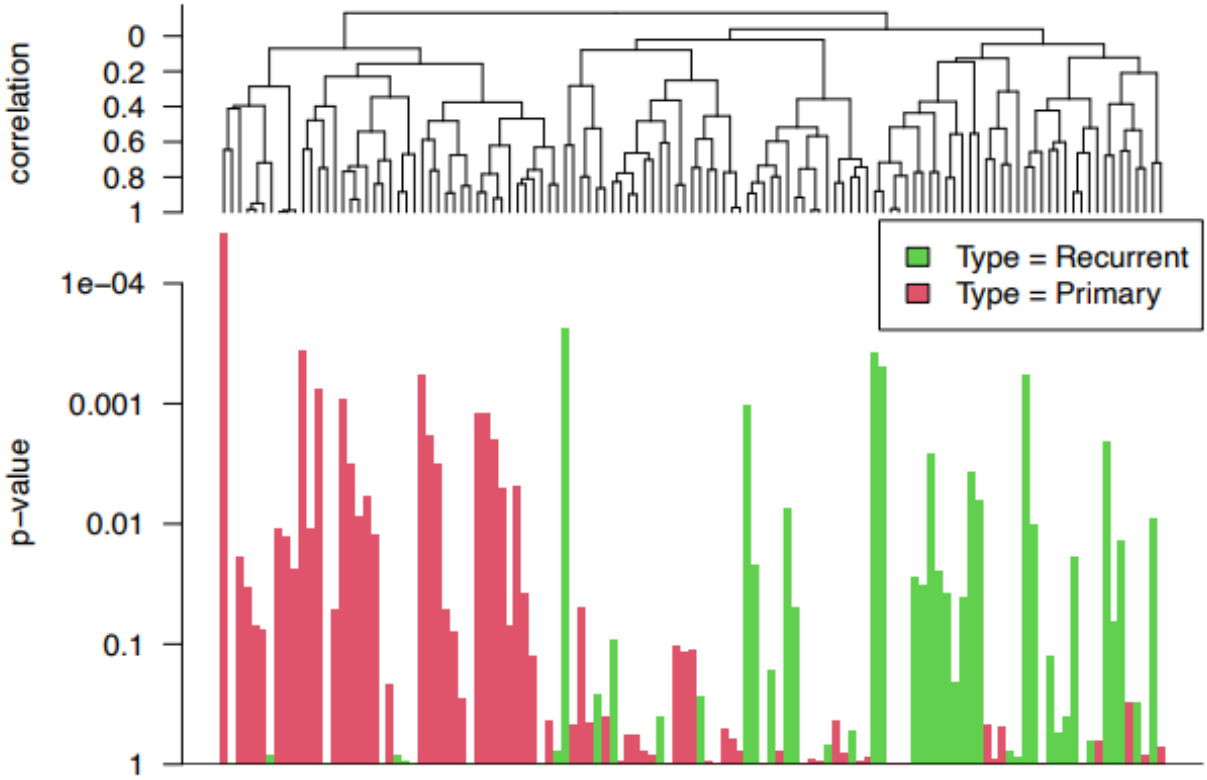

Fig. 3. Gene expression analysis of primary (n = 72) and recurrent ependymoma (n = 47). The dendrogram reveals two distinct groups for which most of the recurrent samples belong to the first group and most of the primary samples to the second group. The samples associated with strong evidence for the association between the response (primary vs recurrent) and the gene expression profile of the gene set (10 genes) have small p-values (tall bars in the bottom plot).

Table 1. Demographic information for patients included for analysis (N = 7; n =3). For five patients (n = 3) ependymoma relapsed after surgical removal and two patients (n = 3) did not experience ependymoma relapse

Age at diagnosis	55.3 ± 39.9 months
Gender	Female (N = 5); Male (N = 2)
Recurrence	Yes (N = 5); No (N = 2)
Tumor location	Posterior fossa (N = 6); Supratentorial (N = 1)
WHO grade	II (N = 4); III (N = 3)
Overall survival	60.1 ± 35.1 months
Status	Alive (N = 4); Death (N = 3)

Table 2. Annotations for significant ions ($p < 0.05$). Fold changes were calculated by dividing the average ion intensity of the *no relapse* group by the average ion intensity in the *eventual relapse* group

m/z	Formula	Adduct	Instrument	Fold change
321.2400	$C_{18}H_{34}O_3$	$[M+Na]^+$	LESA	0.23
145.0293	$C_9H_6O_2$	$[M+H-H_2O]^+$	LESA	1.98
201.0225	$C_8H_{10}O_5S$	$[M+H-H_2O]^+$	LESA	1.64
143.0500	$C_5H_{12}OS$	$[M+Na]^+$	LESA	1.57
170.0609	$C_{11}H_8NO_2$	$[M+H-H_2O]^+$	LESA	1.89
319.2244	$C_{18}H_{32}O_3$	$[M+Na]^+$	LESA	0.45
146.0610	$C_9H_{11}NO_2$	$[M-H-H_2O]^-$	SIMS	2.53
167.0612	$C_{11}H_8N_2$	$[M-H]^-$	SIMS	2.42
160.0402	$C_9H_9NO_3$	$[M-H-H_2O]^-$	SIMS	2.39
145.0293	$C_9H_6O_2$	$[M-H]^-$	SIMS	1.98
158.0610	$C_{10}H_{11}NO_2$	$[M-H-H_2O]^-$	SIMS	2.25
142.0296	$C_9H_7NO_2$	$[M-H-H_2O]^-$	SIMS	1.57
201.0225	$C_8H_{10}O_4S$	$[M-H]^-$	SIMS	1.64
143.0500	$C_{10}H_8O$	$[M-H]^-$	SIMS	2.50
168.0452	$C_{11}H_9NO_2$	$[M-H-H_2O]^-$	SIMS	1.94
170.0609	$C_{11}H_{11}NO_2$	$[M-H-H_2O]^-$	SIMS	1.89
409.057	$C_{21}H_{14}O_9$	$[M-H]^-$	SIMS	0.44
318.1183	$C_{13}H_{23}NO_9$	$[M-H-H_2O]^-$	SIMS	0.49

Table 3. Putative metabolite IDs for significantly affected pathways ($p < 0.05$) between ependymomas which relapsed and those which did not relapse. Pathway analysis was performed using MetExplore (*24*)

Pathway	Putative significant metabolite IDs	Related genes
Tryptophan metabolism	4,6-dihydroxyquinoline; 5-hydroxytryptophol; β-carboline; methyl indole-3-acetate; quinolone-4,8,-diol	ADHFE1, MAOA, MAOB
Linoleate metabolism	12(13)-EpOME / 9(10)-EpOME	EPHX1, EPHX2
Cytochrome metabolism	Coumarin; naphthalene epoxide	CYP2A13, CYP2A6, CYP2F1
Phenylalanine metabolism	L-phenylalanine	DDC, GOT1, GOT2, PAH, TAT
Tyrosine metabolism	1,2-dehydrosalsolinol; 6,7-dihydroxy-1,2,3,4-tetrahydroisoquinoline; adrenochrome	GSTK1

Supplementary Materials

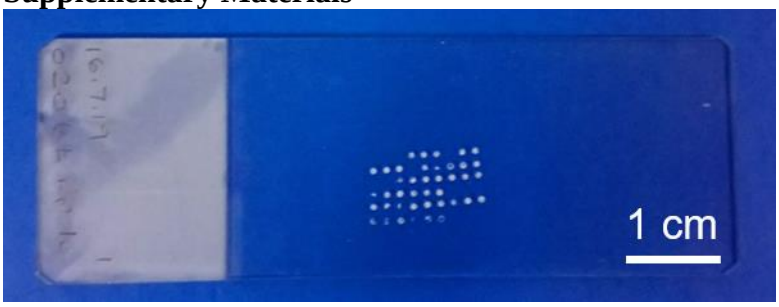

Fig S1: Example of an ependymoma tissue microarray after deparaffinization

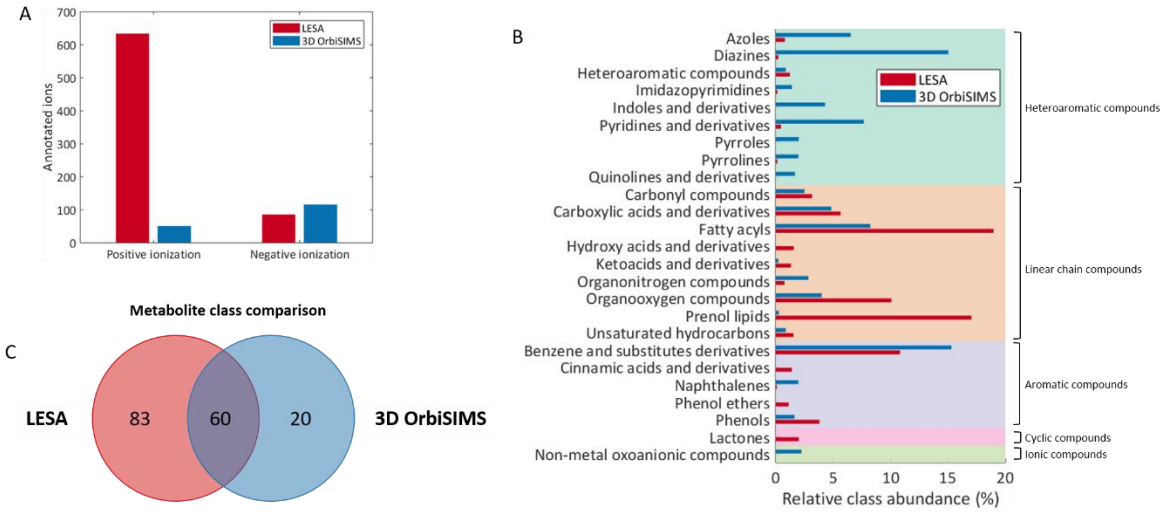

Fig. S2: Identifying putative metabolite features in 3D OrbiSIMS and LESA-MS spectra. (A) In total, more features were identified in the LESA-MS spectra, though the number of mass ions in negative mode identified as metabolite was higher for SIMS. (B) For all identified features, the class as described in the HMDB was obtained to identify which classes can be detected with either technique. The patched areas represent structurally similar classes. (C) From the Venn diagram can be derived that both surface mass spectrometry techniques permit detection of unique metabolite classes (LESA: 83; 3D OrbiSIMS: 20; common classes: 60).

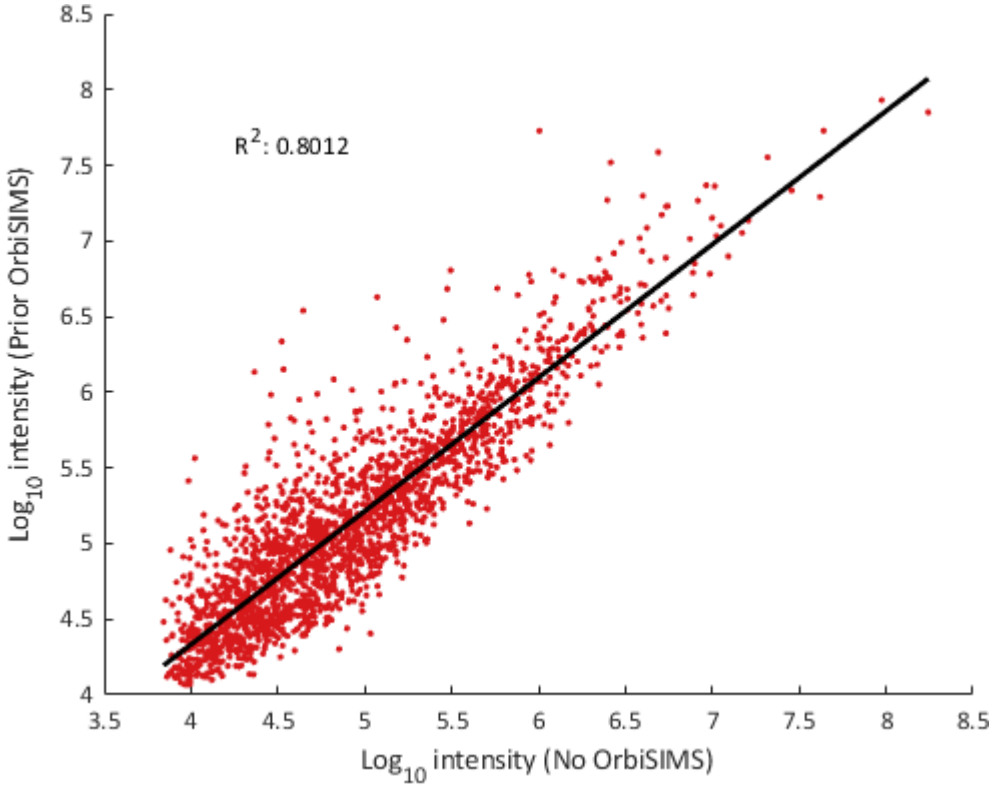

Supplementary Figure 1: Investigating the effect of 3D OrbiSIMS analysis on subsequent LESA-MS/MS analysis. The signal intensity of features identified in LESA-MS spectra did not seem to be affected by prior OrbiSIMS analysis. For one patient (n = 3), the analysis was carried out with and without OrbiSIMS. The scatter plot reveals a good correlation between obtained feature intensities. Furthermore, Student's t-test revealed no significant difference in signal intensity distribution.